Monthly Notices of the ROYAL ASTRONOMICAL SOCIETY

MNRAS **517,** 2567–2576 (2022) https://doi.org/10.1093/mnras/stac2789
Advance Access publication 2022 September 30

QU Vul: An integral field spectroscopy case study of a nova shell

E. Santamaría [1,2]★ M. A. Guerrero [3]★ J. A. Toalá [4] G. Ramos-Larios [1,2] and L. Sabin [5]

[1] *Universidad de Guadalajara, CUCEI, Blvd. Marcelino García Barragán 1421, 44430 Guadalajara, Jalisco, Mexico*
[2] *Instituto de Astronomía y Meteorología, Dpto. de Física, CUCEI, Av. Vallarta 2602, 44130 Guadalajara, Jalisco, Mexico*
[3] *Instituto de Astrofísica de Andalucía, IAA-CSIC, Glorieta de la Astronomía s/n, E-18008 Granada, Spain*
[4] *Instituto de Radioastronomía y Astrofísica (IRyA), UNAM Campus Morelia, Apartado postal 3-72, 58090 Morelia, Michoacán, Mexico*
[5] *Instituto de Astronomía, Universidad Nacional Autónoma de México, Apdo. Postal 877, C.P. 22860 Ensenada, B.C., Mexico*

Accepted 2022 September 23. Received 2022 September 22; in original form 2022 July 11

ABSTRACT

We present GTC MEGARA high-dispersion integral field spectroscopic observations of the nova remnant QU Vul, which provide a comprehensive 3D view of this nova shell. The tomographic analysis of the H α emission reveals a complex physical structure characterized by an inhomogeneous and clumpy distribution of the material within this shell. The overall structure can be described as a prolate ellipsoid with an axial ratio of 1.4 ± 0.2, a major axis inclination with the line of sight of $12^\circ \pm 6^\circ$, and polar and equatorial expansion velocities $\approx$560 km s^{-1} and 400 ± 60 km s^{-1}, respectively. The comparison of the expansion velocity on the plane of the sky with the angular expansion implies a distance of 1.43 ± 0.23 kpc. The ionized mass is found to be $\approx 2 \times 10^{-4}$ M$_\odot$, noting that the information on the 3D distribution of material within the nova shell has allowed us to reduce the uncertainty on its filling factor. The nova shell is still in its free expansion phase, which can be expected as the ejecta mass is much larger than the swept-up circumstellar medium mass. The 3D distribution and radial velocity of material within the nova shell provide an interpretation of the so-called 'castellated' line profiles observed in early optical spectra of nova shells, which can be attributed to knots and clumps moving radially along different directions.

Key words: techniques: imaging spectroscopy – circumstellar matter – stars: individual: QU Vul – novae, cataclysmic variables – ISM: kinematics and dynamics.

1 INTRODUCTION

Classical novae (CNe) outbursts occur on the surface of white dwarfs (WDs) in close binary systems. In these eruptive events the WD (either a carbon–oxygen or an oxygen–neon WD) accretes material from a giant or subgiant low-mass companion star via an accretion disc (Bode & Evans 2008). When the accreted mass reaches critical conditions ($T_{\rm crit} \sim 10^7$ K, $P_{\rm crit} \sim 10^{20}$ dyne cm^{-2}), a thermonuclear runaway (TNR) occurs (Truran & Livio 1986; Gehrz et al. 1998; Starrfield, Iliadis & Hix 2016). The outburst ejects 10^{-5} to 10^{-4} M$_\odot$ (Shafter 2002) at high speeds (Bode 2010). A CN event is characterized by a slow ($\sim$500–2000 km s^{-1}) initial wind followed by a faster (1000–4000 km s^{-1}) wind (Bode & Evans 2008). The interaction of both winds forms a double-shock structure, with the fast wind passing through the slow wind (O'Brien, Lloyd & Bode 1994), producing what is known as a nova remnant. Eventually, the ejected material will expand and disperse into the interstellar medium (ISM).

The 3D physical structure of a nova remnant results from the complex interplay of this slow-wind-fast-wind interaction, when the binary companion orbital energy and angular momentum is transferred to the fast ejecta as it proceeds through the accretion disc and circumstellar material (Livio et al. 1990). The interactions between the ejecta and the companion and accretion disc might produce intrinsically asymmetric ejecta (Livio et al. 1990), with larger (smaller) aspect ratio of the nova remnant for slow (fast) novae (e.g. Slavin, O'Brien & Dunlop 1995; Lloyd, O'Brien & Bode 1997). Images and long-slit spectroscopic observations, interpreted by means of morphokinematic models, can provide 3D views of the physical structure of nova shells (Gill & O'Brien 2000; Santamaría et al. 2022) to test these claims, although the varying conditions of observations for images and spectra, and the limited number of slit positions across the source make not always possible this investigation.

In the last years integral field spectroscopy (IFS) has opened a new window on to our understanding of the morphology, kinematics, 3D physical structure, and properties of nebular shells. Despite the many advantages of IFS observations, there are few works focusing on the study of nova remnants. Woudt et al. (2009) used multi-epoch near-IR images as well as optical Inamori Magellan Areal Camera and Spectrograph (IMACS)-IFS mounted on the 6.5m Magellan Baade telescope to discover a bipolar shell expanding around the helium nova V455 Pup. The observations disclosed a bipolar outflow with expansion velocity of 6720 ± 650 km s^{-1} with a pair of extremely high-velocity knots (8450 ± 570 km s^{-1}) detected at the tips of the bipolar outflows. It is also found that the nova remnant had a narrow waist at earlier times that seems to increase in size with time, thus suggesting an initial density enhancement that preceded the outburst. Its high luminosity made Woudt et al. (2009) also suggest that the WD is massive with a high accretion rate, making it a promising supernova type Ia candidate. Further analysis of the kinematics and emission

★ E-mail: edgar.santamaria8808@alumnos.udg.mx (ES); mar@iaa.es (MAG)

line spectra were presented by Macfarlane, Steeghs & Woudt (2014). Lyke & Campbell (2009) presented multi-epoch observations of the nova V723 Cas spanning four years obtained with the near-IR IFS OSIRIS on Keck II. Interestingly, different emission lines unveiled different morphological features, with the [Si VI] and [Ca VIII] describing an equatorial ring-like structure with a pair of polar knots, whilst the [Al IX] could be attributed to a prolate spheroid structure. The authors suggest that this complex multistructure components can be explained by independent mass ejections. Moraes & Diaz (2009) used Gemini Multi-Object Spectrographs (GMOS) at the Gemini North telescope observations of HR Del to study its morphokinematic and abundances. The line maps exhibit a clumpy shell and confirm the closed hourglass morphology proposed by Harman & O'Brien (2003). Very recently Takeda et al. (2022) presented an analysis of multi-instrument observations of the nova V5668 Sgr. Multi-epoch observations obtained with Keck OSIRIS covering 3 yr were used to study the morphology and expansion pattern of this nova shell. This nova also displays an equatorial structure with a bipolar shape. In particular, it is found that the Brγ emission is not symmetric, which is attributed to an accretion disc.

The studies described above reveal the great potential of IFS observations of nova shells. We present here high-dispersion IFS observations of QU Vul (a.k.a. Nova Vul 1984b) acquired to provide for the first time a complete view of its spatiokinematic properties and 3D physical structure. QU Vul was discovered on 1984 December 22 (Collins et al. 1984) and confirmed afterwards spectroscopically by Rosino & Iijima (1987). It is a peculiar nova with an ONeMg WD (Livio & Truran 1994), implying a unusually massive $\leq$1.0 $M_\odot$ WD (Weidemann 2000). Estimates of the current mass of QU Vul WD are in the range 0.82–0.96 $M_\odot$, which has led to the suggestion that the WD has lost $\sim$0.1 $M_\odot$ (Hachisu & Kato 2016).

The nova reached a maximum visual magnitude of 5.6 mag with a decline time t_2 (i.e. the time it takes to decline 2 mag from the peak brightness; see Gaposchkin 1957) of 20 d (Strope, Schaefer & Henden 2010), becoming one of the brightest fast novae. Its brightness prompted for detailed studies from early stages after its outburst, which has represented an opportunity to know the evolution of the ejected material as well as its spectroscopic properties. Its early photometric and spectral characteristics and their evolution were described by Rosino & Iijima (1987). In a subsequent and more detailed work, Rosino et al. (1992) analysed the spectroscopic properties of the ejecta and confirmed that it conforms the predictions of a TNR event.

According to Rosino et al. (1992), the nova entered the nebular phase early in 1985 April ($t - t_0 \approx 0.25$ yr) and just a few months later its radio continuum emission started showing extended emission ($t - t_0 = 0.79$ and 1.36 yr; Taylor et al. 1987). Extended emission in the optical Hα line was detected a few years later ($t - t_0 =$ 9.54 yr; della Valle et al. 1997), but the first indisputable images of a resolved nebular shell were provided by the *Hubble Space Telescope (HST)* WFPC2 (see Fig. 1) and NICMOS images (Prop. ID 7386, PI F. Ringwald) discussed by Downes & Duerbeck (2000), reporting an ellipsoidal shell with a size of 1.7 × 1.6 arcsec in Hα and 1.6 × 1.3 arcsec at 2.2 μm.[1] The same *HST* NICMOS data were analysed by Krautter et al. (2002), who described the nova as a nearly spherical shell with a radius of 1.07 arcsec. By 2020 the nova

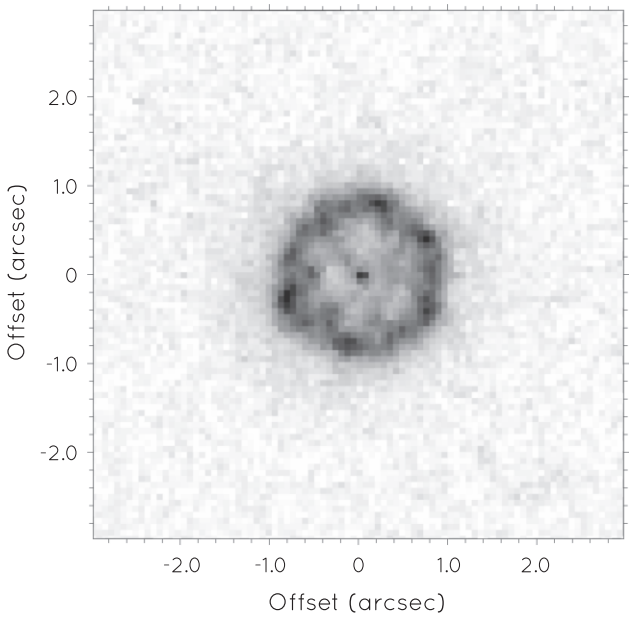

Figure 1. *HST* WFPC2 F656N image of the nebular remnant around QU Vul obtained on 1998 January 1. The nebular shell is clearly resolved with an average radius $\simeq$0.8 arcsec. A faint halo with a radius $\simeq$1.4 arcsec can be hinted in this image. North is up and East to the left.

remnant had expanded up to a radius of 2.1 arcsec (Santamaría et al. 2022).

As for the expansion velocity along the line of sight, Rosino et al. (1992) and della Valle et al. (1997) reported averaged values for the full-width at half-maximum (FWHM) of a number of lines of 1380 km s^{-1} and 1190 km s^{-1}, respectively, whereas Santamaría et al. (2022) measured an expansion velocity of 660 km s^{-1} from the resolved Hα emission line profile. These expansion velocities, in conjunction with the estimates of the angular size, have been used to assess the angular expansion rate and then derive distances of 3.6 kpc (Taylor et al. 1987), 2.6 ± 0.2 kpc (della Valle et al. 1997), 1.7 ± 0.2 kpc (Downes & Duerbeck 2000), 3.14 kpc (Krautter et al. 2002), and 1.4 kpc (Santamaría et al. 2022). In contrast, the distance estimate of $0.90^{+0.35}_{-0.20}$ kpc (Bailer-Jones et al. 2021) based on *Gaia* Early Data Release 3 (EDR3) is smaller than all these expansion distances.

The discrepant expansion velocities and parallax distances[2] emphasize the need for a complete study of the spatiokinematic properties and 3D structure of the nova remnant QU Vul. This has been obtained with the new integral field spectroscopic observations presented here. This work is organized as follows: the observations are presented in Section 2, the results of the data analysis are described in Section 3, and a discussion is given in Section 4. A final summary is presented in Section 5.

2 INTEGRAL FIELD SPECTROSCOPIC OBSERVATIONS

IFS observations of QU Vul were obtained on 2021 August 28 with the Multi-Espectrógrafo en GTC de Alta Resolución para

[1]Their angular radius measurement of 5.6 arcsec based on the subtraction of the stellar PSF to the nebular one on ground-based images most likely probes the wings of the nebular PSF, not the nebular radius.

[2]An even the differing angular sizes derived using the same *HST* NICMOS data by Downes & Duerbeck (2000) and Krautter et al. (2002), which illustrates the problems arising in the selection of the isophotal extent of a nebular shell by different authors.

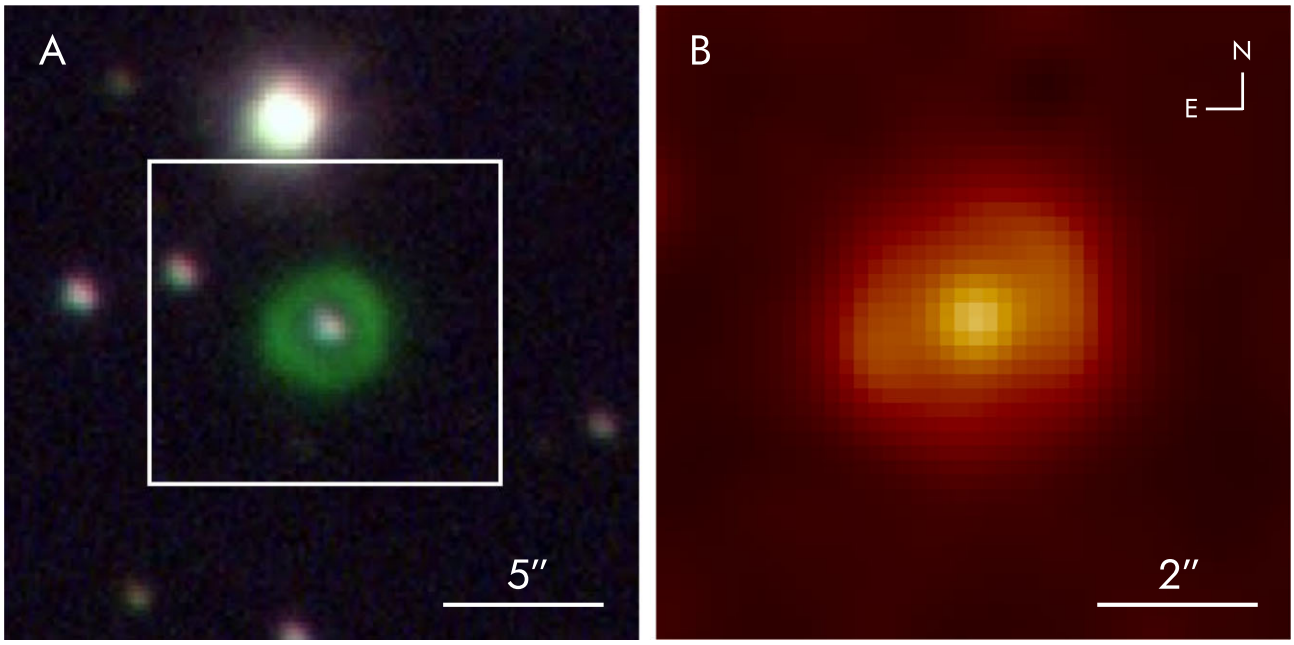

Figure 2. (A) NOT ALFOSC RGB composite picture of the nova QU Vul obtained with g' SDSS λ4800 (blue) and r' SDSS λ6180 (red) broad-band images, and an Hαλ6563 narrow-band (green) image (adapted from Santamaría et al. 2022). The area covered by the GTC MEGARA IFU (12.5 × 11.3 arcsec) is marked by a white rectangle. (B) GTC MEGARA continuum-subtracted Hα image of the nebular emission from QU Vul.

Astronomía (MEGARA; Gil de Paz et al. 2018) attached to the 10.4 m Gran Telescopio Canarias (GTC) at the Roque de los Muchachos Observatory (ORM). We used the Large Compact Bundle (LCB) Integral Field Unit (IFU) mode which provides a FoV of 12.5 × 11.3 arcsec^2 with a 567 hexagonal spaxels[3] of maximal diameter of 0.62 arcsec. The location of the IFU field of view is shown in the left-hand panel of Fig. 2. The observations were carried out with the High-resolution Volume-Phased Holographic (VPH) grism VPH665-HR (centred at 6606 Å), providing a spectral range from ∼6405.6–6797.1 Å and 0.09 Å pix^{-1} with a resolving power of the grating of R = 18, 700 (i.e. ≃16 km s^{-1}). This spectral resolution is suitable to investigate the kinematics of nova shells, with typical expansion velocities ≳500 km s^{-1} (Bode 2010). Three exposures of 600 s were obtained with a seeing of 0.8 arcsec during the observations. All science frames were observed at airmasses of 1.15.

The MEGARA raw data reduction was carried out following the Data Reduction Cookbook (Universidad Complutense de Madrid, Pascual et al. 2019, released version on 2019 July 24). This pipeline applies sky and bias subtraction, flat-field correction, wavelength calibration, spectra tracing, and extraction. The sky subtraction is done using 56 ancillary fibres located ≈2.0 arcmin from the centre of the IFU. The flux calibration was performed using observations of the spectrophotometric standard HR 7950. Finally, the regularization grid task *megararss2cube*[4] was used to produce a final 52 × 58 × 4300 data cube with 0.215 arcsec^2 spaxels.

[3]Single elements of IFUs are referred to as 'spatial pixels' (spaxels), the concept is used to differentiate an IFU spatial component from a detector pixel.

[4]Tool developed by J. Zaragoza-Cardiel available at https://github.com/javierzaragoza/megararss2cube.

3 DATA ANALYSIS AND RESULTS

The GTC MEGARA IFS observations of QU Vul only detect the H α emission line, whose spatial distribution is shown in the continuum-subtracted H α image presented in the right-hand panel of Fig. 2. The H α line profile extracted from a circular aperture 0.5 arcsec in radius encompassing the central star of QU Vul is presented in the top-panel of Fig. 3. For comparison, the H α line profile extracted from NOT ALFOSC long-slit spectroscopic observations (see Santamaría et al. 2022, for a description of the NOT ALFOSC spectroscopic observations) at the location of the star is also presented in the middle panel of the same figure. The stellar H α line profile presents two narrow peaks corresponding to the nebular emission and broad, up to ≈2000 km s^{-1} wings that can be attributed to the accretion disc. Indeed the GTC MEGARA H α line profile of the nebular emission of QU Vul, extracted from an annular region with inner and outer radii 1.6 and 2.2, respectively, does not present these broad wings (Fig. 3-bottom). A multi-Gaussian fit of the stellar H α emission profile has been used to derive the properties of the nebular and stellar components. A number of broad Gaussian profiles is required for the stellar component, whereas the spectral fits to the red- and blue-shifted narrow nebular components imply an expansion velocity along the line of sight ≈560 km s^{-1}. The possible stellar line profile variations between the NOT ALFOSC 2020 July 27 and the GTC MEGARA 2021 August 28 observations might be attributed to the orbital variation of the disc.

The H α line profiles of the stellar and nebular components have been used to extract the channel maps of QU Vul shown in Fig. 4. The nebular emission free from stellar contamination extends approximately from −615 to +665 km s^{-1}. Therefore 28 channel maps with a velocity width ≈45 km s^{-1} have been used to map the H α line, from channel map #2 to #29 in Fig. 4. These channel maps probe different 'velocity layers' of the nova shell, thus providing a tomographic view of QU Vul. Otherwise the first #1 and last #30 channel maps in Fig. 4 show the location of the emission from the central star, thus providing an excellent fiducial point for comparison.

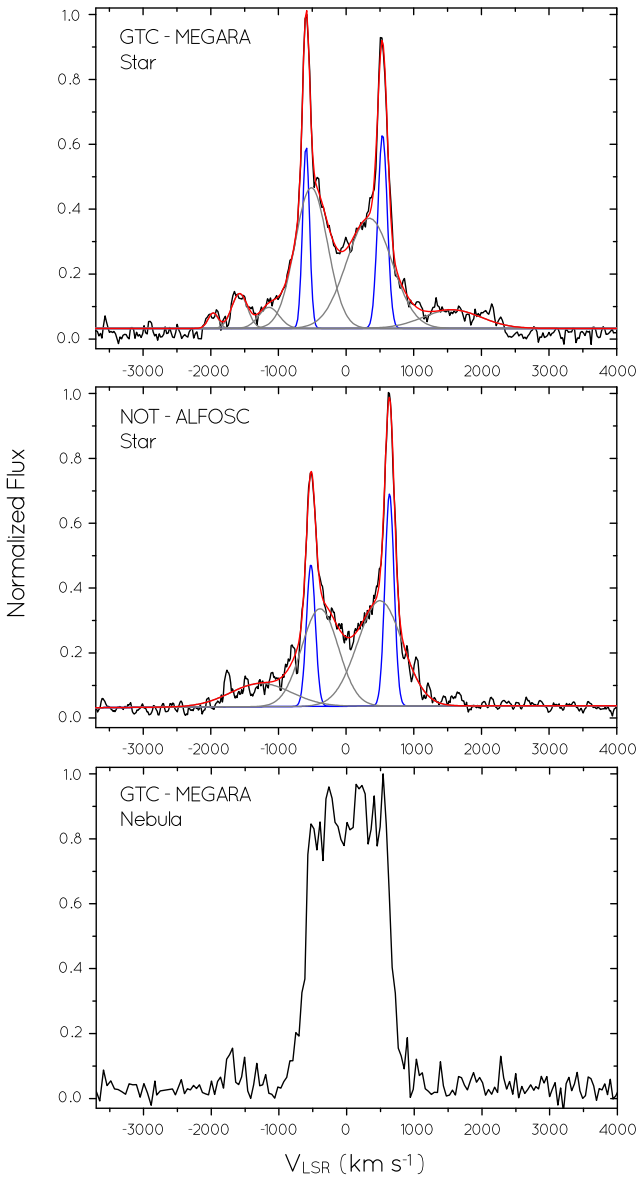

Figure 3. H α emission line profiles of QU Vul detected by GTC MEGARA (top) and NOT ALFOSC (middle) at the position of the central star, and GTC MEGARA nebular emission (bottom). The black line corresponds to the observed profile. The blue and grey lines in the stellar line profiles (top and middle) correspond to multi-Gaussian fits of the narrow nebular and broad stellar components, respectively, whereas the red line represents the total fit to the observed profile. The GTC MEGARA nebular spectrum (bottom) has a flat, 'castellated' top.

Overall these channel maps describe an expanding shell, with small angular size at the velocity tips and a hollow roundish structure in the intermediate velocity channel maps #8 to #21. The shell is not smooth, but it rather shows a number of bright knots connected by fainter filaments. The number and spatial distribution of these knots vary notably among the different velocity channels (check, for instance, the remarkable differences between channels #19 and #22). The shell is neither axially symmetric, with prominent shape variations from one channel to another and with some channels particularly deviating from a circular shape (check, for instance, channels #10, #13, and #15). Interestingly, the intensity peaks of the channels displaying the tips of the shell is not coincident with the position of the central star. The bluest tip of the shell exhibits an offset with respect to the central star ≈0.4 arcsec in channel #3 towards the north-west, whereas the reddest tip in channel #27 has a similar offset along the opposite direction. The shell can therefore be described to be prolate, with its main axis tilted along position angle (PA) ≈123°. This is consistent with the nebular morphology shown in Figs 1 and 2, as well with the claim of asymmetry based on early radio observations (Taylor et al. 1987).

The complexity of the physical structure of QU Vul is illustrated in the position–position–velocity (PPV) diagrams shown in the top and middle panels of Fig. 5. The GTC MEGARA data provide a truly unique 3D view of the H α emission from this nova shell, which is shown from the observer point of view as the image projected on the plane of the sky (left-hand panels), and from the plane of the sky along directions orthogonal and parallel to the main axis (central and right-hand panels). The 3D information is displayed in full detail in the movies available in the online journal as supplementary material.

4 DISCUSSION

The 3D view of QU Vul presented in the previous section reveals its complexity. These data are used next to obtain key information on this nova shell.

4.1 3D Physical structure

The tomographic view of QU Vul shown in Fig. 4 revealed it to be a prolate shell with its main axis aligned along PA ≈123°. This conclusion, which is contrary to the results presented by Santamaría et al. (2022), who concluded that QU Vul could be described as a spherical shell, emphasizes the limitations of long-slit spectroscopic observations compared to IFS observations.

To determine the main geometrical properties of this shell, i.e. its axial ratio and inclination along the line of sight, position–velocity (PV) maps of the H α line have been extracted along selected PAs and compared with synthetic PVs and images of a prolate ellipsoid[5] obtained with the software SHAPE (version 5.0; Steffen & Koning 2017). Since the IFS data allows selecting any PA, the most favourable ones for this comparison have been selected. These are the one along the projection on the plane of the sky of the main axis at PA 123° and that one along its orthogonal direction at PA 303°. The comparison of the observed and synthetic H α line has allowed us to constrain the axial ratio of the prolate shell to 1.4 ± 0.2 and the inclination of its main axis with the line of sight to $12° \pm 6°$. The expansion velocity at the pole is basically the velocity along the line of sight measured from the H α line profile, 560 km s^{-1}, whereas the equatorial velocity, which is also similar to the tangential velocity on the plane of the sky, would be 400 ± 60 km s^{-1}.

4.2 Expansion history

The expansion velocity on the plane of the sky could only be compared with the angular size and age of the nova to obtain its distance if a constant expansion velocity is to be assumed. This is indeed the case of the free-expansion phase observed for a sample of five nova shells with ages up to 130 yr (Santamaría et al. 2020).

[5]Fig. 5 clearly shows that the nova shell QU Vul is not an ellipsoid, but this simple geometrical model will be used to constrain its basic properties: aspect ratio and inclination with the line of sight.

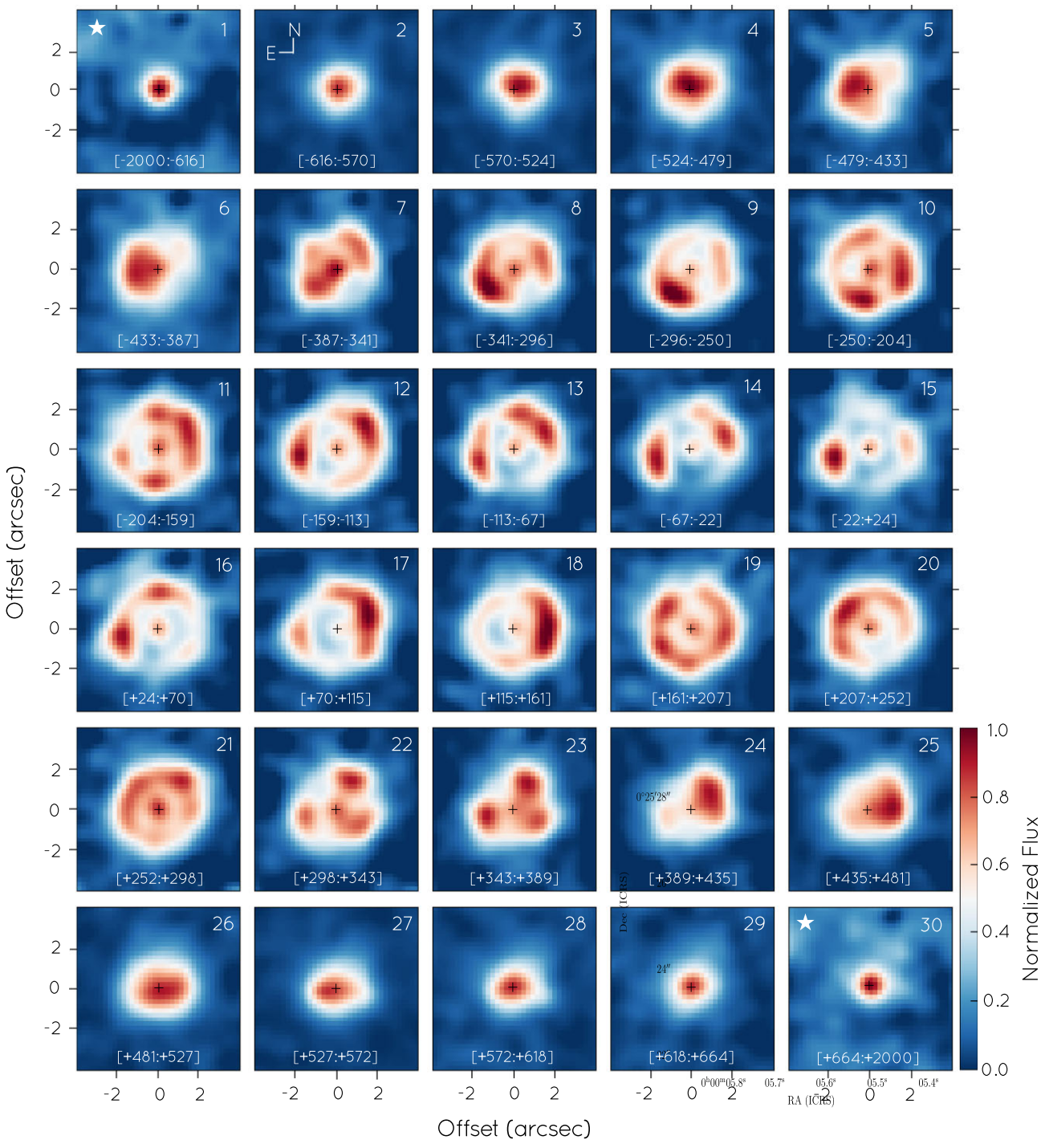

Figure 4. Normalized intensity map channels in the Hα emission line of QU Vul. All channel maps but the first #1 and last #30 cover a velocity range of 45 km s^{-1}. The velocity range of each channel map is labelled at the bottom of each map. The nebular emission spans from channel #2 to #29 from −615 to +665 km s^{-1}. The first #1 and last #30 channel maps show the high-velocity wings of the Hα emission from the central star and had been labelled by a white star. This has been used to mark the star location (black cross) in all channel maps. The line emission from the central star is also detected in channels #7 to #22. North is up and East to the left.

There are, however, many different and not always coherent determinations of the averaged angular expansion rate of QU Vul: 0.080 × 0.047 arcsec yr^{-1} along major and minor axes (at age 1.36 yr; Taylor et al. 1987), 0.099 arcsec yr^{-1} (at age 9.54 yr; della Valle et al. 1997), 0.061 × 0.057 arcsec yr^{-1} (at age 14.0 yr; Downes & Duerbeck 2000), and 0.059 arcsec yr^{-1} (at age 35.7 yr; Santamaría et al. 2022). We note, however, that only the last two measurements resolved the nebular shell, whereas the previous two assumed without further discussion that the intrinsic FWHM of the emission corresponded to the shell radius. If instead the nebular radius of the unresolved shell in the two earlier measurements is equated to one half the separation of two unresolved Gaussians, it

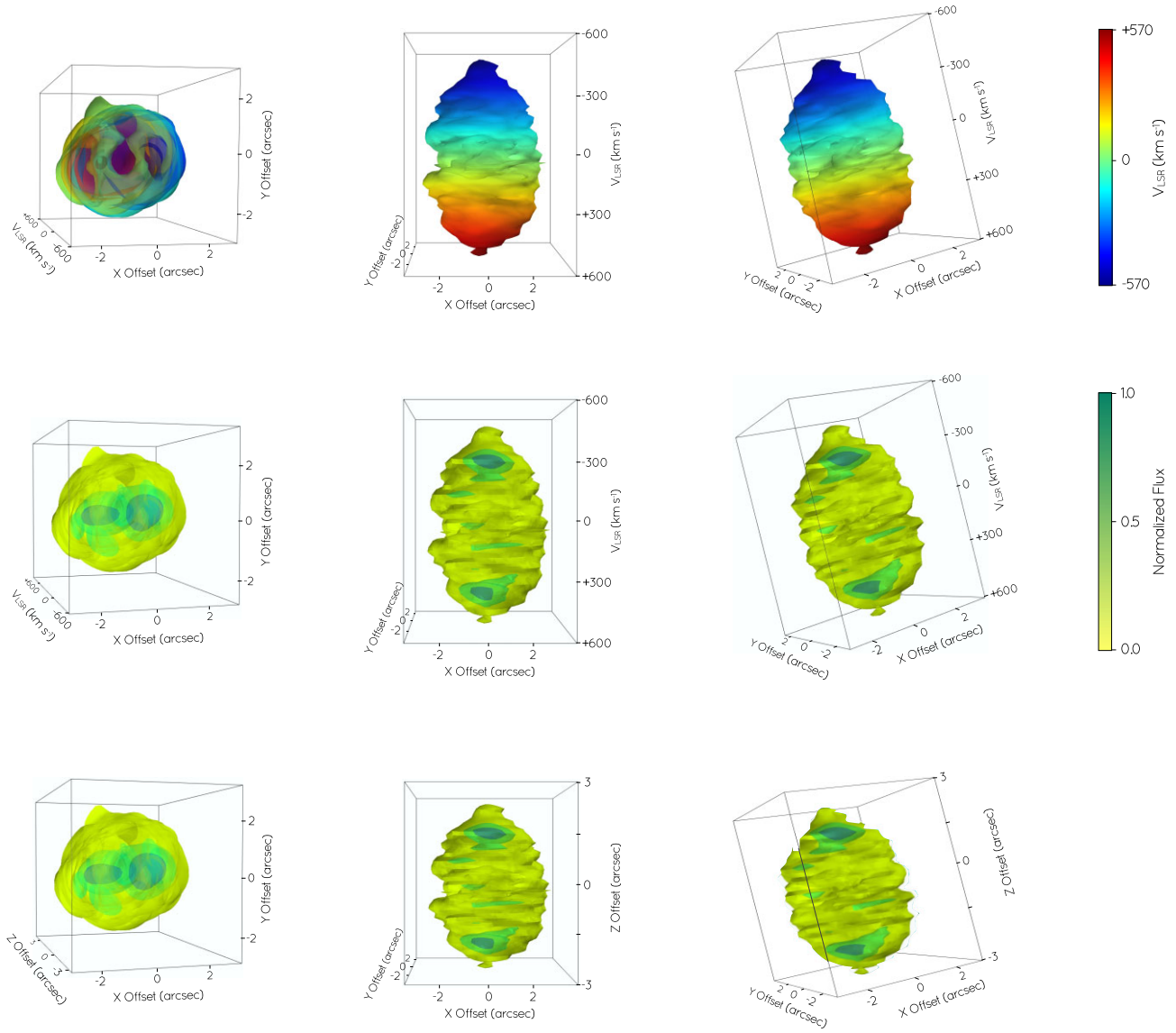

Figure 5. H α emission velocity-coloured (top) and intensity (middle) position–position–velocity (PPV) diagrams of QU Vul, and true 3D intensity distribution (bottom). The left-hand panels show the projection along the observer's point of view (i.e. the direct image), whereas the middle and right-hand panels show the projection from the plane of the sky along directions orthogonal and parallel to the main axis, respectively. The velocity range (top panels) and inhomogeneous distribution of clumps in the nebular remnant (middle and bottom panels) are appreciated in these 3D views of QU Vul.

can be described in terms of the intrinsic FWHM of the source

$$\text{nebular radius} = \frac{\text{FWHM}}{2\sqrt{\ln(2)}} \tag{1}$$

and similar expansion rates of 0.096–0.057 arcsec yr^{-1} (Taylor et al. 1987) and 0.059 arcsec yr^{-1} (della Valle et al. 1997) are obtained. It can thus be concluded that the angular expansion rate of QU Vul has remained constant at a value ≈0.060 arcsec yr^{-1} since its outburst in 1984.

As for the velocity along the line of sight, earlier measurements implied expansion velocities larger than the observed 560 km s^{-1}. Rosino et al. (1992) reported the appearance of a number of blue-shifted absorption components of different lines at −1350, −850, and −680 km s^{-1}. These disappeared soon in the nebular phase and can be interpreted as high-velocity clumps ejected at the time of the nova explosion. Rosino et al. (1992) also derived expansion velocities in the range 1570 to 1380 km s^{-1} for different epochs from the FWHM of a number of emission lines, but for H α, which implied even larger expansion velocities. These results are consistent with those presented by della Valle et al. (1997) with data obtained a few years later that implied expansion velocities of 1190 km s^{-1} also from the FWHM of emission line profiles.

It must be noted that the emission line profiles presented by these authors can be described as 'castellated', i.e. they have a rectangular shape with multiple peaks at the top that resemble the wall and battlements of a castle. This is exactly the same shape of the H α line profile of the whole nebular emission of QU Vul at the bottom of Fig. 3, whose FWHM, ≈1200 km s^{-1}, is similar to the values reported by Rosino et al. (1992) and della Valle et al. (1997). This H α line profile would be the one observed for a spatially unresolved shell (as it is the case of the earliest line profiles of novae, e.g. Iijima et al. 1991). This spectral shape can be interpreted in view of our spatially and spectroscopically resolved data: the 'wall' and its 'battlements' result from the combination of the emission from multiple

knots and filaments moving at different velocities along the line of sight.

The result described above illustrate that the FWHM of the castellated line profiles observed early in the evolution of nova shells should not be used to estimate its expansion velocity. Instead we propose that the bluest and reddest peaks of spatially unresolved castellated profiles should be used to define lower limits for the expansion velocity. The line profiles presented by Rosino et al. (1992) would then indicate that the expansion velocity of QU Vul in 1987 was larger than 420 km s^{-1} and larger than 505 km s^{-1} in 1990. The comparison of these values with the one measured here is thus consistent with a constant expansion velocity for QU Vul along the line of sight.

It must also be remarked that the larger FWHM of the Hα line reported by della Valle et al. (1997) is most likely caused by the contamination of the high-velocity wings of the stellar/disc emission, as illustrated by the comparison of the top and bottom panels in Fig. 3. It is also worth noting that the changes in the castellated profiles described by Rosino et al. (1992) most likely correspond to the brightening and dimming of knots with time caused by shocks in the expanding shell, similar to those observed in SN 1987A (Jakobsen et al. 1991).

4.3 Distance

The free expansion at constant velocity of QU Vul has been found above to be the most simple interpretation of the multi-epoch imaging and spectroscopic observations obtained so far. Therefore the equation

$$\tau = 4750\,\frac{\theta \times d}{v} \qquad (2)$$

relating the age τ in years, the angular radius θ in arcsec, the expansion velocity on the plane of the sky v in km s^{-1}, and the distance d in kpc can be used. For an age of 35.7 yr, the angular radius of 2.1 $\pm$ 0.1 arcsec derived by Santamaría et al. (2022) and the expansion velocity of 400 $\pm$ 60 km s^{-1} presented here imply a distance of 1.43 $\pm$ 0.23 kpc.

The distance derived here is substantially smaller than those previously reported, which are affected by the inappropriate assumptions on the expansion velocity and angular sizes described above. On the other hand, this distance is closer (although still larger) to the one derived from *Gaia* EDR3 of $0.90^{+0.35}_{-0.20}$ kpc (Bailer-Jones et al. 2021), being both distances consistent at 1σ. Note that the determination of *Gaia* distances for stars surrounded by unresolved diffuse emission has been questioned (e.g. Kimeswenger & Barría 2018; Harvey et al. 2020), as red targets with nebular remnant or high-brightness nebulosities show a much larger parallax dispersion, systematically underestimating the errors of objects with circumstellar material in the *Gaia* DR2 data base.

4.4 Time evolution of the Hα luminosity

The Hα luminosity of a nova shell can be expected to decline with time, as the shell expansion implies a decrease in density, while the nova material further cools down. The Hα luminosity of QU Vul has been studied from early stages after its outburst in 1984 and we can compare those with the Hα luminosity estimated in this study to investigate its time evolution.

The first report of the ejecta luminosity (Rosino et al. 1992) implied values for the intrinsic F(Hα) of 7.9 $\times$ 10^{-12} erg cm^{-2} s^{-1} in 1987 August, 3.4 $\times$ 10^{-12} erg cm^{-2} s^{-1} in 1988 September, and

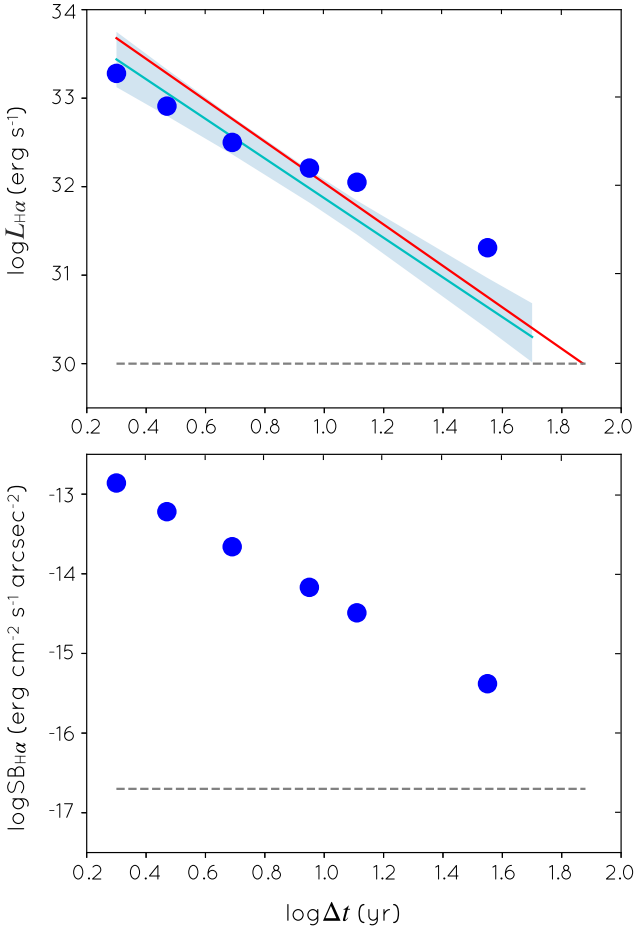

Figure 6. Time evolution of the QU Vul intrinsic Hα luminosity (top) and observed Hα surface brightness (bottom). The red and cyan lines in the top panel describe the time evolution of the intrinsic Hα luminosity derived by Downes, Duerbeck & Delahodde (2001) and Tappert et al. (2020), respectively. The light-blue band in the Tappert et al. (2020) relationship represents the uncertainty described by the authors. The dotted horizontal lines mark the detection limits of the Hα luminosity of 10^{30} erg s^{-1} (top; Downes et al. 2001) and IPHAS surface brightness (bottom; Drew et al. 2005).

1.3 $\times$ 10^{-12} erg cm^{-2} s^{-1} in 1990 August. We note that a value of 5.7 $\pm$ 0.7 has been used for the Hα to Hβ ratio to derive the values listed above. In 1994 August, the intrinsic Hα flux had decreased to 6.8 $\times$ 10^{-13} erg cm^{-2} s^{-1} (della Valle et al. 1997), with an Hα to Hβ ratio of 5.5. The last measurement dates from 1998 January, as obtained by Downes & Duerbeck (2000) using a *HST* Hα image at that time. The intrinsic Hα flux can be worked out to be 2.0 $\times$ 10^{-13} erg cm^{-2} s^{-1}. The intrinsic Hα flux derived from our GTC MEGARA observations is 8.4 $\times$ 10^{-14} erg cm^{-2} s^{-1}. Both this value and that of Downes & Duerbeck (2000) have been corrected from absorption using the extinction value given by Özdönmez et al. (2018) of $E(B-V) = 0.55$ or c(Hβ) = 0.78, which implies a ratio of the observed to the intrinsic Hα flux of 3.6. The present Hα luminosity of QU Vul is thus estimated to be 2.1 $\times$ 10^{31} erg s^{-1}.

The time evolution of the Hα luminosity of QU Vul is shown in the top panel of Fig. 6. The Hα luminosity declines quickly at early times and much more slowly at late times. This behaviour can be compared to that revealed by (the very few) studies of the Hα luminosity evolution of nova shells. Downes et al. (2001) carried out

a detailed study on the behaviour of the H α, H β, and [O III] λ5007 luminosities of nova remnants over time collecting information for a sample of novae of different speed classes. For fast novae, as it is the case of QU Vul, the H α luminosity is derived to vary as:

$$\log L_{\mathrm{H}\alpha} = (34.38 \pm 0.10) - (2.34 \pm 0.11) \log (t - t_0). \quad (3)$$

A more recent investigation of the long-term evolution of the H α and [O III] luminosities of nova shells in comparison with their light curve and nova speed class was presented by Tappert et al. (2020). They propose that the H α luminosity as a function of time can be described by different stages, where it is likely that the evolution of luminosity in the first phases is dominated by shell expansion and changes in volume and density, while in older nova shells the interaction with the ISM takes an important role. Their relationship for the time evolution of the H α luminosity of fast novae is:

$$\log L_{\mathrm{H}\alpha} = (34.11 \pm 0.23) - (2.24 \pm 0.24) \log (t - t_0), \quad (4)$$

which is noted to have a significant scatter ($\sigma = 0.69$). The comparison of the time evolution of the H α luminosity of QU Vul with these relationships in Fig. 6-top shows an excellent agreement. Our measurement of its recent H α luminosity indicates that it might have entered a phase of slower evolution, although the slope of the decay observed in QU Vul is still consistent with the trends reported by Downes et al. (2001) and Tappert et al. (2020) within the uncertainty of these relationships.

The long-term decline of the H α luminosity of QU Vul is obvious in Fig. 6-top. The decline of the H α surface brightness is even deeper in the bottom panel of the same figure (three orders of magnitude in 35 yr), as the nova shell expands with time. This situation raises the question of how long a nova shell would be detectable after the eruption before dissipating in the ISM. After accounting for distances, type of nova, reddening, remnant luminosity, and telescope resolution, Downes et al. (2001) concluded that the lowest H α luminosity in their sample was 10^{30} erg s^{-1}. Meanwhile the detection limit of IPHAS, the INT Photometric H α Survey (Drew et al. 2005), is 2×10^{-17} erg cm^{-2} s^{-1} arcsec^{-2}. These detection limits are plotted in Fig. 6, where it can be foreseen that QU Vul would faint below these at an age $\approx$80 yr, with the flattening of the emission evolution in the last years suggesting a longer visibility time period up to an age of $\approx$200 yr. These are typical ages of nova shells (Sahman et al. 2015).

4.5 Ionized mass and kinetic energy

The ionized mass of a nebula can be determined by estimating its average electron density (N_{e}) from the intrinsic H α flux ($F_{\mathrm{H}\alpha}$) using, for instance, the following expression adapted from Mustel & Boyarchuk (1970):

$$N_{\mathrm{e}} = 1.2 \sqrt{\frac{4\pi d^2 F_{\mathrm{H}\alpha}}{\varepsilon_{\mathrm{H}\alpha} V f}}, \quad (5)$$

where d is the distance to the nebula, V its volume, $\varepsilon_{\mathrm{H}\alpha}$ is the emission coefficient, whose value is 4×10^{-25} erg cm^3 s^{-1} for a plasma at an electron temperature T_{e} of 10 000 K (Boyarchuk et al. 1968), $N_{\mathrm{e}}/N_{\mathrm{p}}$ is assumed to be 1.2, and f is the filling factor. The latter can be described as $f = a \times b$, where the first term a is the fraction of the volume of the shell given by its thickness (i.e. the macroscopic component of the filling factor) and the second term b represents the fraction of the volume covered by condensations (i.e. the microscopic component of the filling factor), which are both smaller than unity. The average electron density of QU Vul would be $370 \times f^{-1/2}$ cm^{-3}.

The total ionized mass of the shell is then computed as:

$$M_{\mathrm{shell}} = \mu\, m_{\mathrm{p}}\, N_{\mathrm{p}}\, V\, f = \mu\, m_{\mathrm{p}} \sqrt{\frac{4\pi d^2 F_{\mathrm{H}\alpha} V f}{\varepsilon_{\mathrm{H}\alpha}}}, \quad (6)$$

where μ is the mean molecular weight, which can be assumed to be 1.44 for a He/H solar ratio. Equation (6) is typically evaluated for the whole shell using its total volume and H α flux, which would imply an ionized mass $\approx 2.4 \times 10^{-4} f^{1/2}\, M_{\odot}$. Very interestingly, the GTC MEGARA IFS observations of QU Vul allow us the possibility to actually evaluate it for each volume element of the 3D data cube. This includes information on the true 3D structure and the inhomogeneous clumpy distribution of the ejected material in the nebular shell (as illustrated in the channel maps shown in Fig. 4), reducing the uncertainty in the macroscopic term a of the filling factor, which is effectively determined. The volume element of the data cube is define by the size of the spatial pixel (0.215 $\times$ 0.215 arcsec) and the wavelength range, which was rebinned to three pixels along the spectral direction (0.27 Å $\approx$ 12 km s^{-1}) to increase the SNR. The latter corresponds to an angular size of 0.065 arcsec, for an ellipsoid with an axial ratio of 1.4, an equatorial radius of 2.1 arcsec, and a polar expansion velocity of 560 km s^{-1}. Accordingly, each data cube element has a volume of 3.0×10^{46} cm^3.

The H α flux of each volume element was corrected from extinction using the factor 3.6 corresponding to a c(H β) extinction coefficient of 0.78 and the distribution of the H α intrinsic intensities and thus of the ionized mass in each volume element computed. The total ionized mass is then obtained by adding the mass in each volume element, which results in a value of $1.9 \times 10^{-4} b^{1/2}\, M_{\odot}$, similar to that reported in previous works (Taylor et al. 1987; Saizar et al. 1992). We emphasize that the ionized mass estimate presented here does not require us to assume a value of the macroscopic component of the filling factor a as the H α flux is directly measured for every volume element of the data cube. Indeed, a comparison of this mass and the average mass computed above implies a value of 0.8 for a.

The ionized mass reported here can be compared with the typical mass ejected in nova outbursts of $\sim 10^{-4}\ M_{\odot}$ (Shafter 2002) for typical values of the microscopic component of the filling factor b in the range 0.1 to unity. The total volume reached by the nova shell implies a swept-up mass of $2.5 \times 10^{-7}\ M_{\odot}$ for an assumed value of 0.55 cm^{-3} for the density of the circumstellar medium (HI4PI Collaboration 2016). The mass of the nova ejecta is indeed much greater than the mass of the swept ISM, by a factor $760 \times b^{1/2}$, which is consistent with its free expansion phase. The latter is also supported by the kinetic energy of QU Vul, $E_{\mathrm{kin}} = 3.1 \times 10^{44}$ erg, which has been derived by adopting an expansion velocity weighted between the radial velocity and the velocity on the plane of the sky. The kinetic energy of nova shells ranges from 10^{43} to 10^{45} erg for slow and fast novae, respectively (Gallagher & Starrfield 1978).

5 SUMMARY

Integral field spectroscopic observations of nova shells have the potential to determine their basic properties and to unveil fine details of their structure, yet very few studies of this type have been carried out so far. Here we present a detailed morphokinematic analysis of the nova shell QU Vul (a.k.a., Nova Vul 1984b) using IFS observations obtained with MEGARA at the GTC.

The observations detect emission only from the H α line, which has been used to obtain a 3D view of the nebula in the position–position–velocity space. This tomographic view reveals that QU Vul can basically be described as a tilted prolate shell with an inhomogeneous

and clumpy structure. A spatiokinematic model to these data, in conjunction with available intermediate-resolution NOT ALFOSC spectra, consisting of a prolate ellipsoid with homologous expansion implies polar and equatorial semiaxes of 2.9 and 2.1 arcsec, respectively, for an axial ratio of 1.4 ± 0.2, an inclination of its main axis with the line of sight at $12^\circ \pm 6^\circ$, and polar and equatorial velocities $\approx$560 km s^{-1} and 400 $\pm$ 60 km s^{-1}, respectively. The position–position–velocity data cube provided by the IFS observations have then been used to obtain the true 3D physical structure of QU Vul.

After checking that the expansion rate of QU Vul since the nova event in 1984 December has been constant at a rate $\approx$0.060 arcsec yr^{-1}, i.e. the nova ejecta is still in its free expansion phase, the tangential velocity in the plane of the sky of 400 ± 60 km s^{-1} has been used to derive a distance of 1.43 ± 0.23 kpc. In checking the possible variation in time of the expansion rate, we note the many discrepant early results on the nebular size and its expansion velocity along the line of sight. The former arise from measurements of angular size from images that do not resolve the nebular shell properly, the latter from the assumption that the FWHM of 'castellated' line profiles can be used to derive the expansion velocity. It is proposed that one half of the velocity separation between the bluest and reddest peaks of line profiles from spatially unresolved nova shells provide a lower limit for its expansion velocity.

The Hα flux measured in the IFS observations has been used to determine an ionized mass for QU Vul of $1.9 \times 10^{-4} M_\odot$. Since this mass is obtained from a 3D data cube, it already accounts for the macroscopic component of the filling factor, for which a value of 0.8 is derived. It is noteworthy to remark that the mass of the ejected material is several hundreds much larger than the mass of the swept-up ISM, which is consistent with a free expansion.

To sum up, this work corroborates the expected potential of IFS observations of nova shells. The overall 3D structure (axial ratio and inclination) and fine details (clumps distribution and shell thickness) of the nova shell of QU Vul have been clearly established and revealed. The 3D structure allows a correct interpretation of the expansion velocity on the plane of the sky and determination of the distance. It also allows interpreting the emission line profiles of unresolved nova shells, which are found to be dominated by the emission from bright clumps moving at different velocities along the line of sight. Finally the 3D information on the distribution of the Hα emission within the nebular shell allows computing the ionized mass without any assumption on the value of the macroscopic filling factor.

ACKNOWLEDGEMENTS

ES acknowledges support from Universidad de Guadalajara and Consejo Nacional de Ciencia y Tecnología (CONACyT) for a student scholarship. MAG acknowledges support of grant PGC 2018-102184-B-I00 of the Ministerio de Educación, Innovación y Universidades cofunded with FEDER funds. GR-L acknowledges support from Universidad de Guadalajara, CONACyT grant 263373 and Programa para el Desarrollo Profesional Docente (PRODEP, Mexico). JAT acknowledges funding from the Marcos Moshinsky Foundation (Mexico) and Dirección General de Asuntos del PersonalAcadémico (DGAPA), Universidad Nacional Autónoma de México, through grants Programa de Apoyo a Proyectos de Investigación e Innovación Tecnológica (PAPIIT) IA101622. LS acknowledges support from PAPIIT grant IN110122. The data presented here were obtained in part with ALFOSC, and provided by the Instituto de Astrofísica de Andalucía (IAA) uder a joint agreement with the University of Copenhagen and NOTSA. The GTC Science Operations team is acknowledged for scheduling the GTC MEGARA observations under the stringent conditions demanded by this program.

The authors are indebted to Drs. Sara Cazzoli and Alessandro Ederoclite for their careful reading of the manuscript and their valuable comments and suggestions.

DATA AVAILABILITY

The data underlying this work are available in the article. The data files will be shared on request to the first author.

REFERENCES

Bailer-Jones C. A. L. et al., 2021, AJ, 161, 147
Bode M. F., 2010, Astron. Nachr., 331, 160
Bode M. F., Evans A., 2008, in Bode M. F., Evans A., eds, Classical Novae, 2nd Edition. Cambridge Astrophysics Series, No. 43. Cambridge Univ. Press, Cambridge, p. 2008
Boyarchuk A. A. et al., 1968, Planet. Nebulae, 34, 162
Collins P. et al., 1984, IAU Circ., 4023
della Valle M., Gilmozzi R., Bianchini A., Esenoglu H., 1997, A&A, 325, 1151
Downes R. A., Duerbeck H. W., 2000, AJ, 120, 2007
Downes R. A., Duerbeck H. W., Delahodde C. E., 2001, J. Astron. Data, 7, 6
Drew J. E. et al., 2005, MNRAS, 362, 753
Gallagher J. S., Starrfield S., 1978, ARA&A, 16, 171
Gaposchkin C. H. P., 1957, Amsterdam, North-Holland Pub. Co. Interscience Publishers, New York, p. 1957
Gehrz R. D. et al., 1998, PASP, 110, 3
Gil de Paz A. et al., 2018, in Evans C. J., Simard L., Takami H., eds, Proc. SPIE Conf. Ser. Vol. 10702, Ground-based and Airborne Instrumentation for Astronomy VII. SPIE, Bellingham, p. 1070217
Gill C. D., O'Brien T. J., 2000, MNRAS, 314, 175
Hachisu I., Kato M., 2016, ApJ, 816, 26
Harman D. J., O'Brien T. J., 2003, MNRAS, 344, 1219
Harvey E. J. et al., 2020, MNRAS, 499, 2959
HI4PI Collaboration, Ben Bekhti N., Flöer L. et al., 2016, A&A, 594, A116
Iijima T. et al., 1991, IAUC, 5236
Jakobsen P. et al., 1991, ApJ, 369, L63
Kimeswenger S., Barría D., 2018, A&A, 616, L2
Krautter J. et al., 2002, AJ, 124, 2888
Livio M., Truran J. W., 1994, ApJ, 425, 797
Livio M. et al., 1990, ApJ, 356, 250
Lloyd H. M., O'Brien T. J., Bode M. F., 1997, MNRAS, 284, 137
Lyke J. E., Campbell R. D., 2009, AJ, 138, 1090
Macfarlane S., Steeghs D., Woudt P., 2014, in Woudt P. A., Ribeiro V. A. R. M., eds, ASP Conf. Ser. Vol. 490, Stellar Novae: Past and Future Decades. Astron. Soc. Pac., San Francisco, p. 115
Moraes M., Diaz M., 2009, AJ, 138, 1541
Mustel E. R., Boyarchuk A. A., 1970, Ap&SS, 6, 183
O'Brien T. J., Lloyd H. M., Bode M. F., 1994, MNRAS, 271, 155
Özdönmez A. et al., 2018, MNRAS, 476, 4162
Pascual S. et al., 2019, in Montesinos B., Ramos A. A., Buitrago F., Schödel R., Villaver E., Pérez-Hoyos S., Ordóñez-Etxeberria I., eds, Proc. XIII Sci. Meeting Spanish Astron. Soc. Vol. 227, Highlights on Spanish Astrophysics X. Spanish Astron. Soc., Salamanca, Spain
Rosino L., Iijima T., 1987, Ap&SS, 130, 157
Rosino L. et al., 1992, A&A, 257, 603
Sahman D. I. et al., 2015, MNRAS, 451, 2863
Saizar P. et al., 1992, ApJ, 398, 651
Santamaría E. et al., 2020, ApJ, 892, 60
Santamaría E. et al., 2022, MNRAS, 512, 2003
Shafter A. W., 2002, in Hameury J.-M., Lasota J.-P., eds, ASP Conf. Ser. Vol. 637, Classical Nova Explosions. Astron. Soc. Pac., San Francisco, p. 462
Slavin A. J., O'Brien T. J., Dunlop J. S., 1995, MNRAS, 276, 353
Starrfield S., Iliadis C., Hix W. R., 2016, PASP, 128, 51001

Steffen W., Koning N., 2017, Astron. Comput., 20, 87
Strope R. J., Schaefer B. E., Henden A. A., 2010, AJ, 140, 34
Takeda L. et al., 2022, MNRAS, 511, 1591
Tappert C. et al., 2020, A&A, 641, A122
Taylor A. R. et al., 1987, A&A, 183, 38
Truran J. W., Livio M., 1986, ApJ, 308, 721
Weidemann V., 2000, A&A, 363, 647
Woudt P. A. et al., 2009, ApJ, 706, 738

SUPPORTING INFORMATION

Supplementary data are available at *MNRAS* online.

Please note: Oxford University Press is not responsible for the content or functionality of any supporting materials supplied by the authors. Any queries (other than missing material) should be directed to the corresponding author for the article.

This paper has been typeset from a TEX/LATEX file prepared by the author.